ACTA STEREOL 1999; 18/2: 131-148
ORIGINAL SCIENTIFIC PAPER

A "RECIPE" FOR ESTIMATING NEURON NUMBER IN THE MAMMALIAN SPINAL CORD USING MODERN STEREOLOGICAL TECHNIQUES

Roger Bjugn[1,2], Maria Hagen[1], Siamak Sadeghi[1] and Jens R. Nyengaard[3]

[1]Department of Anatomy and Cell Biology, University of Bergen,
N-5009 Bergen, Norway,
[2]Department of Pathology, The Central Hospital of Rogaland,
N-4003 Stavanger, Norway, and
[3]Stereological Research Laboratory, University Bartholin Building,
DK-8000 Århus C, Denmark

ABSTRACT

In this review article a brief introduction to the organisation and function of the mammalian spinal cord is given. This short account is followed by a detailed practical approach for estimating the number of neurons, glial and endothelial cells in the grey matter of the spinal cord. All steps, from vascular perfusion fixation, removal of the spinal cord from the spinal column, identification and isolation of individual spinal cord segments, embedding, sectioning, staining, and the final stereological methods and statistical analysis are covered. Focus will be on the practical procedures, and the biological data obtained by these methods will only be discussed with respect to some methodological problems that have been encountered. The possibility of combining specific cell labelling techniques, such as tract tracing and immunocytochemistry, with stereological methods is also discussed, as these methods may solve some of the uncertainties and problems facing neuroscientists who want estimates of neuron number.

Key words: cell count, central nervous system, immunocytochemistry, stereology

INTRODUCTION

The Spinal Cord in General

The spinal cord is the most caudal part of the central nervous system, and its functions are to transmit motor commands to muscles and viscera via the ventral roots of the spinal nerves (Fig. 1), to receive sensory information from the body via the dorsal roots of the spinal cord (Fig. 1), and, finally, to integrate and process certain aspects of the motor and sensory information. In order to protect the soft, vulnerable nervous tissue of the cord from external damage, the spinal cord is located within the vertebral canal of the spinal column. In mammals, the spinal cord usually does not grow as rapidly in length as the spinal column during development, and accordingly does not extend throughout the entire length of the vertebral canal in an adult individual (Ariëns Kappers et al., 1960).

Anatomically, the transition between the spinal cord and the more rostral brain stem occurs where the corticospinal tract makes up the pyramidal decussation. As the pyramidal decussation extends in the rostro-caudal direction, the caudal end of the decussation usually denotes the rostral end of the cord (Clark, 1984). There are, however, no absolute external marks on the cord indicating the caudal limit of the pyramidal decussation, thus making the exact upper end of the cord impossible to define macroscopically. As the rostral limit of the cord is at level with the atlanto-occipital articulation, this easily identifiable articulation usually denotes where the cut separating brain stem and spinal cord is made in practice. The caudal limit of the cord is defined as the end of the most caudal coccygeal segment, where the cord tapers off into the thin filum terminale. In smaller animals it is quite difficult to identify the individual coccygeal segments due to the small size of the spinal nerves, which are used for identifying the individual segments (see Identification and Isolation of Individual Spinal Cord Segments).
The outline of the spinal cord is roughly cylindrical (Fig. 1). Its transverse width is generally greater than its dorso-ventral (or anterior-posterior) width (Ariëns Kappers et al., 1960). The outline of the thoracic part in younger rodents is, however, almost circular. The segments of the cord related to the limbs have a larger circumference, thereby making up the cervical and lumbar enlargements. The size of the two enlargements appears to be associated with the size of the corresponding extremities. However, in most cases the cervical enlargement is the greater (Ariëns Kappers et al., 1960). The spinal nerves with their roots and rootlets give the spinal cord an external segmental arrangement. A segment is usually defined as that part of the cord giving rise to one pair of spinal nerves (Fig. 1). In cross-section, the cord appears with a central core of grey matter and an outer part of white matter (Figs. 1 and 2). The grey matter is usually described as "butterfly"- or "H"-shaped. The relative volume of grey matter in the mammalian spinal cord decreases with increasing species size (Lassek, 1935).

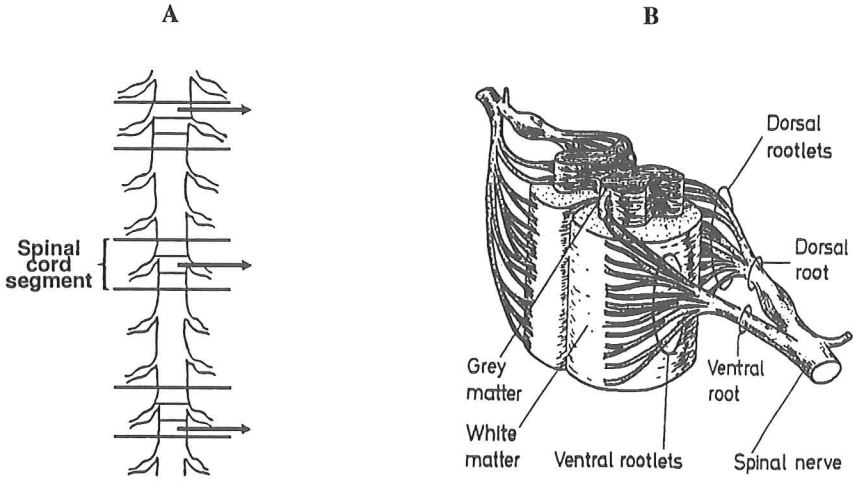

Fig. 1. A: Schematic drawing of part of a mammalian spinal cord showing spinal nerves and spinal cord segments (thick horizontal lines). Arrows indicate how 1-mm-thick transverse slices (thin horizontal lines) are sampled in a random, systematic way for further stereological analysis. B: Schematic drawing of one spinal cord segment and its corresponding spinal nerve rootlets and roots. Part of the white matter has been removed (Modified from Martin, 1989).

Grey Matter

The grey matter contains neurons, glial and endothelial cells. The dorsal horns of the grey matter (Fig. 2A) contain projection (or tract) neurons, which convey sensory information to supraspinal parts of the central nervous system, and interneurons. The middle (or intermediate) zone (Fig. 2A) contains projection neurons, which transmit sensory information to the cerebellum, interneurons and preganglionic autonomic neurons. The ventral horns (Fig. 2A) contain motoneurons, which control the limbs and the trunk, and interneurons (Martin and Jessell, 1991). The term "interneuron" is usually applied to neurons that have axonal projections entirely within the spinal cord. Projection neurons may, however, have collaterals that end within the cord (Burke and Rudomin, 1977). Of the neurons in the spinal cord, the vast majority is believed to be interneurons (Burke and Rudomin, 1977; Willis, Jr. and Coggeshall, 1991). Based on the original observations by Rexed on cytoarchitectural organisation of neurons in grey matter of cat spinal cord (Rexed, 1952; Rexed, 1954), the grey matter can be divided into ten laminae as seen in transverse sections of the cord (Fig. 2b) (see Scheibel, 1984; Schoenen and Faull, 1990; Molander and Grant, 1995). Although somewhat modified in different species and at different levels of the cord, these laminae appear to be similar in all mammals (Clark, 1984; Schoenen and Faull, 1990). The borders of the various laminae are, however, not always easy to distinguish and should be regarded as zones of transition (Molander et al., 1989). The dorsal horns correspond roughly to laminae I-VI. The intermediate part of grey matter is largely made up of lamina VII, while the ventral horns contain laminae VIII, IX and partly VII. Lamina X is the grey matter surrounding the central canal.

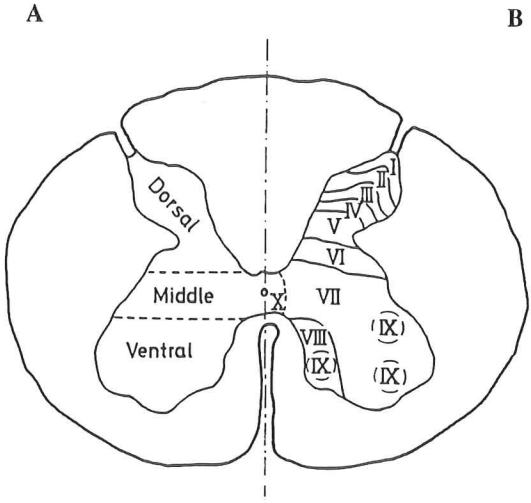

Fig. 2. Schematic drawing of a cross-section of a spinal cord segment showing the dorsal horns, the intermediate matter and the ventral horns (A) in addition to the various Rexed's laminae (B).

Although much remains to be elucidated regarding the functions of the neurons in the various laminae, some of the major tasks are known. Neurons in laminae I and II are mainly concerned with nociception and temperature (Darian-Smith, 1984; Perl, 1984; Martin and Jessell, 1991; Willis, Jr. and Coggeshall, 1991), but also visceral (Réthelyi, 1984; Willis, Jr. and Coggeshall, 1991) and mechanical sensation (Willis, Jr. and Coggeshall, 1991). Neurons in laminae III-IV are involved in mechanoreceptive integration, while those in laminae V-VI integrate pain,

temperature and mechanical sensation (Réthelyi, 1984). The functional differences between laminae III-IV and V-VI are however not clear-cut (see Willis, Jr. and Coggeshall, 1991).

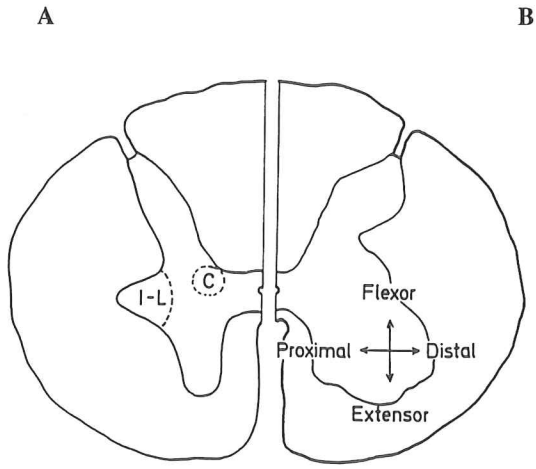

Fig. 3. A: Schematic drawing of a cross-section of a thoracic spinal cord segment showing the intermediolateral nucleus (I-L) of the lateral horn and Clarke's nucleus (C). B: Schematic drawing of a cross-section of a lumbar spinal cord segment showing how the motoneurons are located with respect to which muscle groups they innervate.

Lamina VII contains neurons (Clarke's column or nucleus; see Fig. 3A) which transmit mechanoreceptive information to the cerebellum. These neurons are only located in the thoracic and upper lumbar segments of the cord (Kaas, 1990; Tracey, 1995). Lamina VII also contains the intermediolateral nucleus with its sympathetic preganglionic neurons (Fig. 3A). A similar column in two or three sacral segments contains the parasympathetic preganglionic neurons of the cord. Lamina VIII contains interneurons related to skeletal muscle control (Martin and Jessell, 1991). Lamina X contains neurons concerned with nociception and visceral sensation (Willis, Jr. and Coggeshall, 1991). Lamina IX contains somatic motoneurons, which in general can be divided into two main groups: a ventromedial group innervating the axial muscles of the body and a dorsolateral group innervating the limbs (Fig. 2b). Both groups are made up of columns of neurons several segments long. The ventromedial group is found in almost the entire cord, while the dorsolateral group is located in the lower cervical and upper thoracic segments and in the lumbar segments of the cord (Ghez, 1991). In man, some authors divide the somatic motoneurons into four separate groups (see Schoenen and Faull, 1990).
Three different kinds of somatic motoneurons are described: Alpha-motoneurons, which innervate extrafusal muscle fibres, gamma-motoneurons, which innervate intrafusal muscle fibres, and beta-motoneurons, which innervate both extra- and intrafusal muscle fibres (Burke and Rudomin, 1977). Most of the motoneurons are assumed to be of the gamma type, among which the alpha-motoneurons are scattered. Motoneurons innervating proximal muscles are generally located more medially while those innervating more distal muscles are located progressively more laterally. Motoneurons innervating extensor muscles are situated more ventrally than those innervating flexor muscles (Ghez, 1991) (Fig. 3B).

White Matter

The white matter contains the various fibre tracts in the spinal cord. The white tinge seen in fresh specimens is due to the numerous myelin sheaths. Glial and endothelial cells are the most numerous cells in white matter. However, a particular group of neurons is also located in the white matter (Clark, 1984; Jansen and Loewy, 1997). These neurons project to sympathetic preganglionic neurons (Jansen and Loewy, 1997). The transition between grey and white matter is quite distinct when viewed at low-power magnification. However, at higher magnification the border may be somewhat fuzzy.

MATERIAL AND METHODS

The following notes are based on our experience on spinal cords from adult mouse, rat, rabbit, cat and man, and on developing mouse and rat spinal cords.

Anesthesia

The choice of anesthesia for experimental animals must be decided in collaboration with the local laboratory animal science specialist, and in accordance with the specific national regulations. In our laboratory, we use a mixture of midazolam and fentanyl /fluanison which is injected subcutaneously in the neck. The anesthetics certainly affect neuronal function, whether they also affect structure is, to our knowledge, unknown. It is, however, highly unlikely that they will affect cell number if the spinal cord is vascular perfusion fixed immediately after adequate anesthesia has been obtained.

Vascular Perfusion Fixation

After opening the thorax, a cannula connected to the perfusion fluids is introduced into the aorta via the left ventricle. As soon as the perfusate is flowing into the general circulation, the right atrium is cut open. Whether to use vasodilators, heparin, cold fixative, fixative at room temperature or at body temperature, to rinse with saline or a buffer before the aldehyde containing fixative is introduced must be decided by the individual researcher. Artificial respiration is usually not considered necessary if the vascular perfusion starts less than 1 min after opening the thorax (Descarries and Schröder, 1968). In our opinion, the choice of vascular perfusion technique most probably does not affect the total number of cells estimated later on, if the counting is based on the presence of cell nuclei, as the nuclear material is quite well preserved independent on the fixation procedure. However, if identification of cells is based on cytoplasmic morphology or immunostains, the choice of perfusion method surely will affect the estimated number of a particular cell type. The well preserved morphology obtained by a high perfusion flow using a 2-4% glutaraldehyde-containing fixative must be weighed against the brief fixation using a low glutaraldehyde concentration usually necessary for immunocytochemical protocols.

Spinal Cord Extraction

After skinning the perfused animal, we remove the dorsal axial musculature, including the neck muscles, using scissors and dental scrapes. All individual spinal vertebra can then be identified. The spinal cord and the brain stem are separated by a cut between the atlas and the occipital bone. Using bone rongeurs and/or scissors (Fine Science Tools, Heidelberg, Germany), we remove the most dorsal part of the vertebral arches. If the bone is especially thick, we remove the spinous processes and part of the vertebral arches using a small hand drill with a spherical burr. All dorsal root ganglia and the most proximal part of the corresponding spinal nerves on both sides of the cord are then identified and isolated using microscissors. This rather

time-consuming task is done with the aid of a stereomicroscope. The remaining lateral parts of the vertebral arches are then removed. In our experience, such a procedure ensures that none, or only a very few, spinal roots are torn. Only in a few cases we have been able to surely identify a first cervical dorsal root ganglion. The second dorsal root ganglion, situated between the atlas and the axis, represents our reference point for further identification of individual spinal cord segments. In the lower thoracic and in the lumbosacral part of the cord, the dorsal root ganglia are situated rather far away from the spinal cord, and care must be taken not to severe the roots when removing bone and musculature.

If only the lumbosacral part of the cord is to be used, we identify the sacral bone and the lowermost lumbar vertebra. After removing the vertebral arches, the lowermost lumbar dorsal root ganglion is identified and serves as the reference for the identification of other spinal cord segments.

Before the spinal cord with all the dorsal root ganglia can be fully isolated, the dura has to be loosened from the bone. Special care has to be taken in the upper cervical part in order not to damage the spinal roots, as the dura is strongly attached to the vertebrae in this area. Dissection of the coccygeal spinal nerves is particular demanding in small animals due to the small diameters of the nerve roots and the possibilities of mechanical damage to the roots and dorsal root ganglia during the dissection procedure. In some cases, especially in embryos and neonatal animals, we have only been able to isolate and identify the spinal cord segments down to the lumbar segments. During the entire dissection procedure, one should regularly keep the tissue moist using a buffer.

Adams and Murray (1982) have given an excellent description of the practical procedure for removing the spinal cord and the dorsal root ganglia in man. They recommend the anterior approach. In our experience, the posterior approach makes identification of spinal nerves easier. It is quite beneficial to isolate and identify one or two spinal nerves before the entire spinal cord is removed. Care must be taken when the saw cut is performed on the vertebral pedicles so that the spinal roots or the spinal cord is not injured. The cervical spinal cord is the most demanding part to remove. A long neck incision, which clearly will be seen afterwards, is necessary. In some cases ethical considerations therefore inhibits the removal of the upper cervical segments in man.

Identification and Isolation of Individual Spinal Cord Segments

After isolating the spinal cord, the dura has to be opened carefully using (micro)scissors, in order to identify the individual spinal cord segments. We usually open the dura from the dorsal side. In the cervical and the upper thoracic cord, the spinal roots leave the spinal cord in a rather acute angle. In the lower thoracic cord and in the lumbosacral cord, the roots have an oblique course and are closely related to the spinal cord surface in the first part of their course. Isolating individual spinal cord segments by cutting midway between the rootlets belonging to consecutive spinal nerves (Fig. 1A), accordingly demands a careful dissection procedure in the lower spinal cord. In smaller animals we use razor blades for cutting. In larger animals and man, a scalpel is used. Variations with respect to segmental levels between corresponding right and left spinal nerves and corresponding dorsal and ventral roots exist. In man, rootlets may actually anastomose between consecutive spinal nerves (Pallie, 1959; Barson and Sands, 1977). We have made similar observations in the lumbosacral region of the rat spinal cord. However, in our experience, such differences are of minor practical importance. Length measurements of the entire spinal cord using a stereomicroscope on individual segments or parts of the spinal cord (e.g., the cervical part) reveal quite small variations between animals.

Selection of Segments for further Stereological Analysis

In our initial studies on rat and mouse spinal cord, the individual segmental borders were ignored and we cut oblique slices several segments long for embedding (Bjugn, 1993; Bjugn and Gundersen, 1993). However, knowing the exact segmental level is crucial in some settings, and defining borders between the dorsal horns, intermediate part, and the ventral horns and between various laminae (Fig. 2) is far more easy in transverse sections than in oblique sections. We have therefore modified our procedure, and now identify and isolate all individual spinal cord segments before cutting transverse slices (Bjugn et al., 1997).

How many segments should be selected for further stereological analysis? Based on simulations for estimating the coefficient of error depending on the number of segments included, we recommend that approximately 10 (8-12) segments are included if the entire spinal cord is to be analysed. For most animal species, this means that every third segment should be selected in a systematic random fashion. Usually, we exclude the first cervical spinal segment, as the architecture of this segment is somewhat special (see Molander and Grant, 1995; Jansen and Loewy, 1997). From each segment chosen, we cut an approximately 1-mm-thick transverse slice. As the spinal cord segments may be several mm long, it is necessary to sample these 1-mm-thick slices in a random fashion to avoid bias in the sampling procedure (see Fig. 1A).

If only part of the spinal cord is being investigated (e.g., the lumbar part), the number of sampled slices should generally be 5-10 (Bjugn et al., 1997).

Embedding

The transverse slices are placed in ordinary plastic processing cassettes, as used for routine paraffin embedding, dehydrated in ethanol (70% x 2, 90% x 2, and 99% x 2; one hour in each bath), infiltrated in 2-hydroxyethyl methacrylate (Technovit®, Heraeus Kulzer, Wehrheim, Germany; 12 hours in each bath) before final embedding in 2-hydroxyethyl methacrylate. Final embedding is done in plastic embedding moulds suitable for glycol methacrylate, and special stubs for direct microtome attachment are embedded at the same time (e.g., Agar, Stansted, England). If the tissue slices are very small, the slices are embedded in 5% Agar (prior to dehydration) in order to get a proper orientation during embedding and to make handling easier during infiltration and embedding. Dehydration and infiltration is done at 4°C while embedding is done at room temperature.

If immunocytochemical procedures are to be undertaken, it may be advantageous to avoid plastic infiltration and instead infiltrate the sections in 5-30% sucrose before cryosectioning. To ensure stability of the tissue during sectioning, we usually embed the tissue in a mixture of egg albumin, gelatine and glutaraldehyde before attaching the specimen to the freezing platform using Tissue-Tek.

Sectioning

To get 35-µm-thick plastic sections (the set cutting thickness); the block surface has to be moistened with water in order to avoid cracking during sectioning. The practical minimun section thickness for using the optical disector is, in our opinion, approximately 25 µm. The real section thickness of the final stained and covered histological section can be measured using a microcator (see Equipment for Stereological Analysis). For sectioning, we prefer glass Ralph-knives, but various kinds of steel knives can also be used. The section is removed from the knife edge using a fine brush and placed in a water bath in order to unfold the section before being mounted on a glass slide by means of a brush. The section is then dried at 60°C.

Table 1. An example of how to estimate the total volume of the ventral grey matter of an adult rat spinal cord and the coefficient of error (CE=SD/mean) of this estimate. The measured height of the spinal cord segments is h, and P_i is number of points hitting the ventral grey matter on the histological sections using test points.

Segment	h (mm)	P_i	$P_i \bullet P_i$	$P_i \bullet P_{i+1}$	$P_i \bullet P_{i+2}$
C1	2.5				
C2	2	36	1296	1512	1728
C3	2.3				
C4	2				
C5	2.3	42	1764	2016	966
C6	2.1				
C7	2.5				
C8	2	48	2304	1104	672
T1	2				
T2	2.7				
T3	1.8	23	529	322	391
T4	2				
T5	2.3				
T6	3	14	196	238	280
T7	3				
T8	2.4				
T9	3.4	17	289	340	646
T10	2.5				
T11	2.2				
T12	3.4	20	400	760	1080
T13	3.5				
L1	3.5				
L2	2.5	38	1444	2052	950
L3	2.7				
L4	2.7				
L5	2.3	54	2916	1350	
L6	2.4				
S1	2.1				
S2	2.2	25	625		
S3	2.7				
S4	2.8				
Sum	$\sum h = 77.8$	$\sum P_i = 317$	A = 11763	B = 9694	C = 6713

Table 1, contd.

The area associated to each test point (a/p= P) in the volume estimate is $22.3 \bullet 10^{-3}$ mm^2. The estimated mean height of the spinal cord segments ($\bar{h}$) is the total height of the spinal cord (Σh) divided by the total number of segments (=31), i.e., (77.8 / 31) mm = 2.51 mm. F (=3) is the sampling fraction of segments chosen for area estimation. The total volume of the ventral grey matter is then calculated as:

$$V(ref) = F \bullet \bar{h} \bullet (a / p) \bullet \Sigma P_i = 3 \bullet 2.51 \text{ mm} \bullet 22.3 \bullet 10^{-3} \text{ mm}^2 \bullet 317 = 53.2 \text{ mm}^3 \quad (1)$$

The coefficient of error of the volume estimate (CE[V(ref)]) is calculated from the three equations given below (Gundersen et al., 1998):

$$\text{Noise} = 0.0724 \bullet \left(b/\sqrt{a}\right) \bullet \sqrt{n_S \bullet \Sigma P} = 0.0724 \bullet 18 \bullet \sqrt{10 \bullet 317} = 73 \quad (2)$$

where 0.0724 is a constant, $b/\sqrt{a}$ is the "average profile shape" of the grey matter ventral horns in the spinal cord (see Gundersen and Jensen, 1987) and n_S is the total number of sections (=10).

$$\text{Var}(\Sigma a) = \frac{3(A - \text{Noise}) - 4B + C}{240} = \frac{3(11763 - 73) - 4 \bullet 9694 + 6713}{240} = 13 \quad (3)$$

where Var(Σa) is the variability of the area estimates of the histological sections and A, B and C originate from the first part of Table 1 (see above).

$$CE[V(ref)] = \frac{\sqrt{\text{Noise} + \text{Var}(\Sigma a)}}{\Sigma P_i} = \frac{\sqrt{73 + 13}}{317} = 0.03 \quad (4)$$

Cryosectioning

For cryosectioning, a special cryo sledge microtome with automatic cooling of the stage, or an ordinary sledge microtome with a modified stage allowing cooling of the tissue with dry ice, is used. An ordinary C-steel knife for paraffin sectioning yields excellent results. The section thickness is usually set at minimum 50 µm as the final section thickness usually shrinks to about half of the set thickness.

Staining

Whatever stain used, it is advisable to make some staining trials and check the penetration of the stain if 2-hydroxyethyl methacrylate is used for the first time. For nervous tissue, we usually use a modified Giemsa-stain (see Table 2 in Braendgaard et al., 1990). Some useful leaflets regarding staining can be obtained from the producers of 2-hydroxyethyl methacrylate.

Covering Microscopy Slides

The choice of mounting medium is not crucial. However, we advise some mechanical pressure on the cover slips after mounting. In some cases it appears that a thick tissue section in

combination with a thick layer of mounting medium may cause problems when focusing through the section using a high-magnification lens (x60 or x100) with high numerical aperture.

Storage of 2-hydroxyethyl methacrylate Sections
As some stains will fade quite substantially if exposed to sunshine, it is advisable to keep the microscopy slides in a cool, dark place.

Equipment for Stereological Analysis
Our observations on the histological sections are made using a modified Olympus BX50 microscope with a microcator (Heidenhain ND 281, Traunreut, Germany) and a motorised specimen stage (Märzhäuser EK-8, Wetzlar, Germany) with an object rotator (Olympus, Denmark; see Fig. 9 in Gundersen et al., 1988b). This special object rotator makes it possible to rotate the histological section freely on top of the specimen stage. A video camera, connected to a monitor, is mounted on top of the microscope. By means of the C.A.S.T.-Grid software program (version 1.09, Olympus, Denmark), the motorised stage is controlled and the appropriate stereological frames are generated and superimposed upon the image of the histological sections viewed on the monitor.

Stereological Techniques
Estimating tissue volume (reference volume):
Areas of the various parts of the grey and white matter on the transverse sections are estimated by point counting on the histological sections. We usually aim at about 150-200 points altogether at the individual tissue compartment in question (accordingly; 450-600 points if both the cervical, thoracic, and lumbar grey matter volumes are to be estimated separately). The volumes of the various tissue compartments are then calculated by multiplying the cross-sectional area with the measured distance between the sections (see above and Tbl. 1). Note that this volume estimate is not unbiased. An unbiased estimate can only be made if the Cavalieri's principle is followed for tissue sampling (Gundersen and Jensen, 1987; Bjugn et al., 1997). The latter approach renders, however, some difficulties with respect to tissue sampling if the segmental identification is the most important issue. In our experience, not using Cavalieri's principle does not cause any significant systematic error with respect to the volume estimates.

Estimating numerical densities:
Numerical densities of the various cell categories (that is, the number of cells in a certain volume of tissue) are estimated by means of an optical disector (Gundersen et al., 1988a; Bjugn, 1993; Bjugn and Gundersen, 1993). We usually keep the depth of the disector at 15 µm (measured by a microcator). When counting both neurons and glial and endothelial cells, we now use two different counting frames. The disector frame area for counting neurons (and unidentified cells) is usually kept 3-4 times bigger than the frame used for counting glial cells and endothelial cells. The exact size of the frame areas and the X- and Y-step lengths for the motorised specimen stage distance used for a systematic random sampling of fields of vision on the histological sections, must be decided on by the particular experiment in question.

Estimating total number of cells:
The total number of neurons and number of glial and endothelial cells are then estimated by multiplying the numerical densities with the corresponding reference volume (see above and Tbl. 2).

Statistical Analysis

In Tbl. 1 we give an example of how the total ventral grey matter volume was estimated, using original observations on rat spinal cord. In Tbl. 2 we demonstrate how the total number of neurons was estimated using the same spinal cord as in Tbl. 1. A detailed description of how to estimate the coefficient of error for both the volume estimate (Tbl. 1), the estimate of numerical density of neurons (Tbl. 2), and the estimate of total number of neurons (Tbl. 2) is also provided.

DISCUSSION

In our experience, it is not the application of stereological principles and techniques that may cause concern with respect to the estimation of the number of neurons, glial and endothelial cells in the spinal cord. We believe it is the still unsolved general biological question about identification of particular cell types which is of major concern. Part of this problem may, however, be resolved using specific cell labelling techniques.

Identification of Cells

Deciding upon reliable criteria for neuron identification in the spinal cord is still a matter of debate, as it is for estimating number of neurons in other parts of the CNS (Evans, 1990) (see also Delineation of Laminae and Specific Neuronal Nuclei). Functionally, the large majority, but not all, neurons are characterised by their ability to generate action potentials and thereby make signalling between different neurons possible (Kandel, 1991). Glial cells, as far as we know, cannot do this. By electrophysiological techniques, it is accordingly possible to distinguish between neurons and glial cells. Morphologically, neurons are generally recognised by their distinct Nissl bodies in the cytoplasm and large, spherical nuclei containing a prominent nucleolus. In the dorsal horns of the spinal cord, smaller neurons may have only scant or no cytoplasm (Palay and Chan-Palay, 1977) and a pale nucleus with marked indentations (Nathaniel and Nathaniel, 1966; Todd, 1990). Although a number of, perhaps most, such cells contain a prominent nucleolus in the nucleus indicating that they are neurons (Palay and Chan-Palay, 1977), it is not always easy to make unambiguous decisions on whether a condensation in the nucleus is «prominent». It may accordingly be difficult, or even impossible, to distinguish such neurons from astrocytes (Palay and Chan-Palay, 1977).

It has been stated that neurofilaments is a characteristic feature of neurons (Palay and Chan-Palay, 1977) (see also Peters et al., 1991). Several different neurofilaments have been characterised (see Darnell et al., 1990). The three most widely known antibodies to such filaments are the 68kD (or 70kD), 150kD (or 160kD) and 200kD (or 210kD) neurofilament antibodies. However, small neurons only have limited, if any, neurofilament proteins (see Schlaepfer, 1987; Wolf et al., 1996). The neuron-specific enolase is not specific for neurons (see Lowe and Cox, 1990; Wolf et al., 1996), and S-100 is found in both neurons and glial cells (see Goto et al., 1988). Calcineurin, a calmodulin binding protein, appears to be quite specific for neurons in the central nervous system (Goto et al., 1986), but antibodies against calcineurin does not stain all neurons (Goto et al., 1986; Goto et al., 1987). Chromogranins are glycoproteins associated with neurosecretory granules. However, their detection in formaldehyde fixed material has been somewhat unsatisfactory (see Wolf et al., 1996). Synaptophysin is a membrane glycoprotein, which is localised in presynaptic vesicles, whereas there is no consistent labelling of neuronal somas (see Wolf et al., 1996).

Table 2. An example of estimating the total number of neurons in the ventral part of the grey matter of spinal cord in the same rat as used in Table 1. Q_i^- is the number of neurons counted in the optical disectors at each segmental level included. The coefficient of error (CE=SD/mean) of the number estimate is estimated in Eqs. 6-9.

Segment	Number of disectors	Q_i^-	$Q_i^- \bullet Q_i^-$	$Q_i^- \bullet Q_{i+1}^-$	$Q_i^- \bullet Q_{i+2}^-$
C1					
C2	14	8	64	200	136
C3					
C4					
C5	25	25	625	425	450
C6					
C7					
C8	32	17	289	306	170
T1					
T2					
T3	19	18	324	180	648
T4					
T5					
T6	10	10	100	360	200
T7					
T8					
T9	22	36	1296	720	1152
T10					
T11					
T12	24	20	400	640	580
T13					
L1					
L2	26	32	1024	928	384
L3					
L4					
L5	35	29	841	348	
L6					
S1					
S2	18	12	144		
S3					
S4					
Sum	Σ#(dis) = 225	$\Sigma Q_i^- = 207$	A* = 5107	B* = 4107	C* = 3720

Tbl.2, contd.

$\sum Q_i^-$ is the total number of neurons counted in the optical disectors, a(dis) is the area of the disector frame (=4147•10^{-6} mm^2), $\sum$#(dis) is the number of disectors hitting grey matter, h(dis) is the height of the disector (=0.015 mm) and V(ref) is the total ventral grey matter as estimated in Tbl. 1. Using Eq. 5, the total number of neurons is then estimated:

$$N(\text{neurons}) = \frac{\sum Q_i^-}{a(\text{dis}) \bullet \sum \#(\text{dis}) \bullet h(\text{dis})} \bullet V(\text{ref}) \tag{5}$$

$$= \frac{207}{4147 \bullet 10^{-6}\,\text{mm}^2 \bullet 225 \bullet 0.015\,\text{mm}} \bullet 53.2\,\text{mm}^3 = 782 \bullet 10^3$$

The CE of the estimate of total neuron number is made up of two contributing factors; the estimate of ventral grey matter volume (reference volume), and the estimate of numerical density of neurons. The CE of the reference volume is estimated in Eqs. 2-4 in Tbl. 1. The CE of the numerical density of neurons is estimated as shown in Eqs. 6-8 below (Gundersen et al., 1998):

$$\text{Noise} = \sum Q_i^- = 207 \tag{6}$$

$$\text{Var}(Q_i^-) = \frac{3(A^* - \text{Noise}) - 4B^* + C^*}{240} = \frac{3(5107 - 207) - 4 \bullet 4107 + 3720}{240} = 8 \tag{7}$$

where A*, B* and C* originate from the first part of Tbl. 2 (see above).

$$CE\left[N_V(\text{neurons})\right] = \frac{\sqrt{\text{Noise} + \text{Var}(\sum Q_i^-)}}{\sum Q_i^-} = \frac{\sqrt{207 + 8}}{207} = 0.07 \tag{8}$$

The CE of the estimated total number of neurons is then calculated using Eq. 9:

$$CE\left[N(\text{neurons})\right] = \sqrt{CE\left[V(\text{ref})\right]^2 + CE\left[N_V(\text{neurons})\right]^2} = \sqrt{0.03^2 + 0.07^2} = 0.08 \tag{9}$$

A recently described monoclonal antibody reacting against a DNA-binding neuron-specific protein called NeuN (*Neu*ronal *N*uclei) (Mullen et al., 1992; Wolf et al., 1996; Kuhn et al., 1996; Peterson et al., 1996; Jansen and Loewy, 1997; Ling et al., 1997), appears more promising from a stereological point of view. It appears to bind specifically to neurons, with the exception of Purkinje cells in the cerebellum, is quite resistant to formaldehyde fixation and other processing steps, and binds to the cell nuclei, which is ideal for stereological studies aiming at estimating neuron number. A paper applying this antibody in combination with the disector technique has already been published (Peterson et al., 1996).

In our opinion, neuron number estimates should always be used cautiously, as neither purely morphological methods nor immunocytochemical techniques render unambiguous neuron identification. However, total cell number estimates will not be affected by this problem of identification of various cell types. We accordingly recommend that total cell number should be estimated in addition to the estimates of specific cell numbers.

In the spinal cord, numerous studies have aimed at estimating the number of motoneurons. Although the "larger size" of motoneurons is often used to identify motor nuclei and their motoneurons, studies of retrogradely filled motoneurons in the rat spinal cord have found soma diameters ranging from 10 to 65 µm (Peyronnard et al., 1986; Swett et al., 1986; Crockett et al., 1987), values quite similar to that of the entire neuron population in the ventral horns. Clearly, soma size alone can not be used to differentiate between motoneurons and other types of neurons in the spinal cord. However, the combination of tract-tracing techniques and stereological methods should be able to make more precise estimates of the number of motoneurons.

Delineation of Laminae and Specific Neuronal Nuclei

As stated in the introduction, the borders of the various laminae in the spinal cord are not always easy to distinguish and should be regarded as zones of transition (Molander et al., 1989). Similarly, identification of specific nuclei in the spinal cord, as elsewhere in the central nervous system, may not always be clear-cut. Quite often, such distinctions are based on particular stains and neuronal cytoarchitecture. But, what happens if the "large, angular neurons typical of nucleus X" is absent, or appears markedly reduced in number in the experimental animals, compared to the control animals? Does this imply that neurons in "nucleus X" have died? It could well happen that these neurons undergo morphological changes, but retain their function. Accordingly, the overall delineation of the nucleus will be affected (Fig. 4), and surely the estimated total number of neurons. An interesting debate on this topic can be found in the July number of Trends in Neurosciences in 1997 (1997;20:343-346).

The opposite could also happen, that the neurons lose their function, but retain their morphology. The biological problem of identifying particular tissue borders and correlating neuronal morphology with neuronal function will surely affect the results obtained whatever the soundness of the stereological approach. Note that this biological problem is not solved by using the fractionator (Gundersen et al., 1988a) for estimating neuron number (See Volumetric Changes). The fractionator only solves the problems of volumetric tissue changes *per se*, and will not solve the problem of identifying particular tissue borders or possible changes in neuronal morphology.

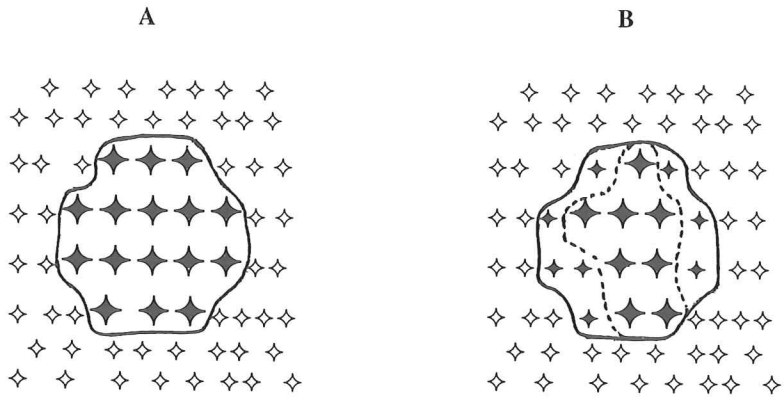

Fig. 4. Schematic drawing of a hypothetical "nucleus X" characterised by "large, angular neurons" as observed in control animals (A; black neurons within continuos line). If the neurons undergo morphological changes as a result of the experimental setting, and the same morphological criteria are applied, the outline of the nucleus and the estimated total number of such neurons in the experimental animals will be affected (B; black neurons within stippled lines), even though the neurons in reality may retain their number and function (B; black neurons within continuos line).

Volumetric Changes

The one technical problem we will focus on using plastic sections, are changes in tissue volume, changes which most probably occur during fixation, dehydration, embedding, and sectioning. The area of individual tissue samples (both longitudinally and transversely cut) can be measured and compared after fixation, after embedding, and finally after sectioning and staining. Ordinarily, the tissue shrinks from fixed to embedded state. After sectioning, staining and covering, the tissue area is usually back to fixation state. However, both larger and smaller areas have been recorded. When occurring, less than 10-15% volumetric change is the rule. The procedures appearing to be crucial, are the sectioning and the drying step (Gerrits et al., 1987). One disadvantage using cryosections is that the cryosection height usually is reduced down to 50% or less after staining and final mounting. The real height must therefore be checked carefully using a microcator during microscopy.

As volumetric changes during tissue processing can affect the results obtained (except when using the fractionator technique for number estimation (Gundersen et al., 1988a), we recommend that some time be spent on estimating shrinkage. However, one should bear in mind that it could be possible that various compartments within the tissue undergo volumetric shrinkage different from the overall shrinkage of the entire tissue block – so-called "differential shrinkage".

Conclusion

We believe that combining the described stereological methods with specific cell labelling techniques is one way of obtaining more reliable quantitative data on neuron number in the spinal cord.

ACKNOWLEDGEMENTS

The assistance of the technical staff at the Stereological Research Laboratory, University of Aarhus and Ms. Edith Fick at the Department of Anatomy and Cell Biology, University of Bergen is greatly appreciated. The financial support of the Nordic Academy for Advanced Study, Leo Nielsen's Foundation, Foundation for Research in Neurology, Geert Jørgensen's Foundation, Lundbeck Foundation and the Norwegian Research Council is greatly appreciated.

REFERENCES

Adams JH, Murray MF. The spinal cord. Atlas of post-mortem techniques in neuropathology. Ch. 4. Cambridge: Cambridge University Press, 1982: 67-81.

Ariëns Kappers CU, Huber GC, Crosby EC. The comparative anatomy of the spinal cord. The comparative anatomy of the nervous system of vertebrates, including man, Vol. 1. Ch. 2. New York: Hafner Publishing Company, 1960: 135-334.

Barson AJ, Sands J. Regional and segmental characteristics of the human adult spinal cord. J Anat 1977; 123:797-803.

Bjugn R. The use of the optical disector to estimate the number of neurons, glial and endothelial cells in the spinal cord of the mouse - with a comparative note on the rat spinal cord. Brain Res 1993; 627:25-33.

Bjugn R, Gundersen HJG. Estimate of the total number of neurons and glial and endothelial cells in the rat spinal cord by means of the optical disector. J Comp Neurol 1993; 328: 406-11.

Bjugn R, Nyengaard JR, Rosland JH. Spinal cord transection - No loss of distal ventral horn neurons. Modern stereological techniques reveal no transneuronal changes in the ventral horns of the mouse lumbar spinal cord after thoracic transection. Exp Neurol 1997; 148:179-86.

Braendgaard H, Evans SM, Howard CV, Gundersen HJG. The total number of neurons in the human neocortex unbiasedly estimated using optical disectors. J Microsc 1990; 157: 285-304.

Burke RE, Rudomin P. Spinal neurons and synapses. In: Kandel ER, ed. Handbook of Physiology. Section 1: The nervous system. Vol. I. Cellular biology of neurons, Part 2. 2. ed. Ch. 24. Maryland: American Physiological Society, 1977: 877-944.

Clark RG. Anatomy of the mammalian cord. In: Davidoff RA, ed. Handbook of the spinal cord. Vol. 2 & 3. Anatomy and physiology. Ch. 1. New York: Marcel Dekker, 1984: 1-45.

Crockett DP, Harris SL, Egger MD. Plantar motoneuron columns in the rat. J Comp Neurol 1987; 265:109-18.

Darian-Smith I. Thermal sensibility. In: Darian-Smith I, ed. Handbook of Physiology. Section 1: The nervous system. Vol. III. Sensory processes, Part 2. 2. ed. Ch. 19. American Physiological Society, Maryland, 1984: 879-913.

Darnell J, Lodish H, Baltimore D. Actin, myosin, and intermediate filaments: Cell movements and cell shape. Molecular cell biology. 2. ed. Ch. 22. New York: Scientific American Books, 1990: 859-902.

Descarries L, Schröder JM. Fixation du tissu nerveux. J Microscopie 1968; 7:281-6.

Evans SM. Stereological investigation of the ageing of human cerebral neocortex (Thesis). Liverpool: University of Liverpool, 1990.
Gerrits PO, van Leeuwen MBM, Boon ME, Kok LP. Floating on a water bath and mounting glycol methacrylate and hydroxypropyl methacrylate sections influence final dimensions. J Microsc 1987; 145:107-13.
Ghez C. The control of movement. In: Kandel ER, Schwartz JH, Jessell TM, eds. Principles of neural science. 3. ed. Ch. 35. New York: Elsevier, 1991: 533-47.
Goto S, Matsukado Y, Mihara Y, Inoue N, Miyamoto E. The distribution of calcineurin in rat brain by light and electron microscopic immunohistochemistry and enzyme-immunoassay. Brain Res 1986; 397:161-72.
Goto S, Matsukado Y, Miyamoto E, Yamada M. Morphological characterization of the rat striatal neurons expressing calcineurin immunoreactivity. Neuroscience 1987; 22: 189-201.
Goto S, Matsukado Y, Uemura S, Mihara Y, Inoue N, Ikeda J, Miyamoto E. A comparative immunohistochemical study of calcineurin and S-100 protein in mammalian and avian brains. Exp Brain Res 1988; 69:645-50.
Gundersen HJG, Bagger P, Bendtsen TF, Evans SM, Korbo L, Marcussen N, Møller A, Nielsen K, Nyengaard JR, Pakkenberg B, Sørensen FB, Vesterby A, West MJ. The new stereological tools: Disector, fractionator, nucleator and point sampled intercepts and their use in pathological research and diagnosis. APMIS 1988a; 96:857-81.
Gundersen HJG, Bendtsen TF, Korbo L, Marcussen N, Møller A, Nielsen K, Nyengaard JR, Pakkenberg B, Sørensen FB, Vesterby A, West MJ. Some new, simple and efficient stereological methods and their use in pathological research and diagnosis. APMIS 1988b; 96:379-94.
Gundersen HJG, Jensen EB. The efficiency of systematic sampling in stereology and its prediction. J Microsc 1987; 147:229-63.
Gundersen HJG, Jensen EBV, Kieu K, Nielsen J. The efficiency of systematic sampling in stereology - reconsidered. J Microsc 1998 (in press).
Jansen ASP, Loewy AD. Neurons lying in the white matter of the upper cervical spinal cord project to the intermediolateral cell column. Neuroscience 1997; 77:889-98.
Kaas JH. Somatosensory system. In: Paxinos G, ed. The human nervous system. Ch. 24. San Diego: Academic Press, 1990: 813-44.
Kandel ER. Nerve cells and behaviour. In: Kandel ER, Schwartz JH, Jessell TM, eds. Principles of neural science. 3. ed. Ch. 2. New York: Elsevier, 1991: 18-32.
Kuhn HG, Dickinson-Anson H, Gage FH. Neurogenesis in the dentate gyrus of the adult rat: age-related decrease of neuronal progenitor proliferation. J Neurosci 1996; 16:2027-33.
Lassek AM. A comparative volumetric study of the gray and white substance of the spinal cord. J Comp Neurol 1935; 62:361-76.
Ling C, Zuo M, Alvarez-Buylla A, Cheng MF. Neurogenesis in juvenile and adult ring doves. J Comp Neurol 1997; 379:300-12.
Lowe J, Cox G. Neuropathological techniques. In: Bancroft JD, Stevens A, eds. Theory and practice of histological techniques. 3. ed. Ch. 17. Edinburgh: Churchill Livingstone, 1990: 343-78.
Martin JH. Neuroanatomy. Text and atlas. New York: Elsevier, 1989: 1-483.
Martin JH, Jessell TM. Anatomy of the somatic sensory system. In: Kandel ER, Schwartz JH, Jessell TM, eds. Principles of neural science. 3. ed. Ch. 25. New York: Elsevier, 1991: 353-66.
Molander C, Grant G. Spinal cord cytoarchitecture. In: Paxinos G, ed. The rat nervous system. 2. ed. Ch. 2. San Diego: Academic Press, 1995: 39-45.

Molander C, Xu Q, Rivero-Melian C, Grant G. Cytoarchitectonic organization of the spinal cord in the rat: II. The cervical and upper thoracic cord. J Comp Neurol 1989; 289:375-85.
Mullen RJ, Buck CR, Smith AM. NeuN, a neuronal specific nuclear protein in vertebrates. Development 1992; 116:201-11.
Nathaniel EJH, Nathaniel DR. Fine structure of the neurons of the posterior horn in the rat spinal cord. Anat Rec 1966; 155:629-42.
Palay SL, Chan-Palay V. General morphology of neurons and neuroglia. In: Kandel ER, ed. Handbook of physiology. Section 1: The nervous system. Vol. I. Cellular biology of neurons, Part 1. Ch. 2. Maryland: American Physiological Society, 1977: 5-37.
Pallie W. The intersegmental anastomoses of posterior spinal rootlets and their significance. J Neurosurg 1959; 16:188-96.
Perl ER. Pain and nociception. In: Darian-Smith I, ed. Handbook of Physiology. Section 1: The nervous system. Vol. III. Sensory processes, Part 2. 2. ed. Ch. 20. American Physiological Society, Maryland, 1984: 915-75.
Peters A, Palay SL, Webster HD. The neuronal cell body. The fine structure of the nervous system. Neurons and their supporting cells. 3. ed. Ch. 2. New York: Oxford University Press, 1991: 14-69.
Peterson DA, Lucidi-Phillipi CA, Murphy DP, Ray J, Gage FH. Fibroblast growth factor-2 protects entorhinal layer II glutamatergic neurons from axotomy-induced death. J Neurosci 1996; 16:886-98.
Peyronnard JM, Charron LF, Lavoie J, Messier JP. Motor, sympathetic and sensory innervation of rat skeletal muscles. Brain Res 1986; 373:288-302.
Rexed B. The cytoarchitectonic organization of the spinal cord in the cat. J Comp Neurol 1952; 96:415-95.
Rexed B. A cytoarchitectonic atlas of the spinal cord in the cat. J Comp Neurol 1954; 100:297-379.
Réthelyi M. Synaptic connectivity in the spinal dorsal horn. In: Davidoff RA, ed. Handbook of the spinal cord. Vol. 2 & 3: Anatomy and physiology. Ch. 4. New York: Marcel Dekker, 1984: 137-77.
Scheibel AB. Organization of the spinal cord. In: Davidoff RA, ed. Handbook of the spinal cord. Vol. 2 & 3. Anatomy and physiology. Ch. 2. New York: Marcel Dekker, 1984: 47-77.
Schlaepfer WW. Neurofilaments: Structure, metabolism and implications in disease. J Neuropathol Exp Neurol 1987; 46:117-29.
Schoenen J, Faull RLM. Spinal cord: Cytoarchitectural, dendroarchitectural, and myeloarchitectural organization. In: Paxinos G, ed. The Human Nervous system. Ch. 2. Academic Press, 1990: 19-53.
Swett JE, Wikholm RP, Blanks RH, Swett AL, Conley LC. Motoneurons of the rat sciatic nerve. Exp Neurol 1986; 93:227-52.
Todd AJ. An electron microscope study of glycine-like immunoreactivity in laminae I-III of the spinal dorsal horn of the rat. Neuroscience 1990; 39:387-94.
Tracey DJ. Ascending and Descending Pathways in the Spinal Cord. In: Paxinos G, ed. The Rat Nervous System. 2. ed. Ch. 5. San Diego: Academic Press, 1995: 67-80.
Willis WD, Jr. , Coggeshall RE. Functional organization of dorsal horn interneurons. Sensory mechanisms of the spinal cord. 2. ed. Ch. 5. New York: Plenum Press, 1991: 153-215.
Wolf HK, Buslei R, Schmidt-Kastner R, Schmidt-Kastner PK, Pietsch T, Wiestler OD, Blümcke I. NeuN: A useful neuronal marker for diagnostic histopathology. J Histochem Cytochem 1996; 44:1167-71.